

NUTRIENT TRANSPORT IN BEACHES SUBJECTED TO FRESHWATER INPUT AND TIDES

*Michel C. Boufadel**
Environmental Engineering and Science Department
Clemson University
P.O. Box 340919
Clemson, SC, 29634-0919

Makram T. Suidan, Christian H. Rauch, Chang-Hoon Ahn
Department of Civil and Environmental Engineering
University of Cincinnati
Cincinnati, Ohio 45220

Albert D. Venosa
U.S. Environmental Protection Agency
National Risk Management Research Laboratory
Cincinnati, OH 45269

** Corresponding author: Research Assistant Professor. Ph: (864) 656-5574, Fax: (864) 656-0652, Email: mboufad@clemson.edu.*

ABSTRACT: *Bioremediation of oil spills on beaches commonly involves the addition of nutrients to stimulate the growth of indigenous oil-degrading bacteria. The selection of the best application strategy of nutrients requires an understanding of the physical factors affecting beach hydraulics and hydrodynamics. We investigated these factors here using a laboratory beach and a numerical model that is able to simulate density-dependent flows in two-dimensional variably-saturated media. We found that beach geometry plays a major role in beach hydraulics and hydrodynamics because the flow lines are perpendicular to the beach surface. Under tidal action, we found that seawater enters the beach from the top and causes the entrapment of less saline water in the beach. Guidelines for the selection of the best application strategy of nutrients are provided.*

Keywords: *Salinity, Interface, Finite Element, Nutrients, Bioremediation*

Introduction

Bioremediation is an emerging technology for restoration of oil-contaminated beaches (Merlin et al., 1995). Biostimulation, which is a form of bioremediation, involves the addition of nutrients, such as nitrogen and phosphorus, which might exist in nature in limiting concentrations, to enhance the growth rate of indigenous hydrocarbon-degrading bacteria (Venosa et al., 1996). The effectiveness of biostimulation depends on contact between the added nutrients and the oil-polluted zone, which is usually less

than about 25 cm below the beach surface (Rosenburg et al., 1992). Ideally, nutrient concentrations in contact with the oil should be sufficient to support maximal growth rate of the oil-degrading bacteria, and this concentration must be maintained for the longest possible time. Therefore, maximizing the residence time of the nutrients in the contaminated zone of the beach is an important goal for bioremediation.

Many approaches have been developed to maintain contact between oil and nutrients, including lipophilic and slow-release nutrient formulations. However, most slow-release and many lipophilic fertilizers rely on dissolution of the nutrients into the aqueous phase before they can be used by hydrocarbon degraders (Safferman, 1991). Thus, design of effective oil bioremediation strategies and nutrient delivery systems requires an understanding of the transport of water-soluble fertilizer in the beach.

Dissolved nutrients are expected to move with the water in the beach sand. Water flow through the porous matrix of a beach is driven by a combination of three main factors. The first factor that affects water flow in beaches is wave action. This operates through the mechanism of runup-rundown (Riedl and Machan, 1972; Brown and McLachlan, 1990). At wave runup water enters the beach and percolates vertically through the unsaturated zone until it reaches the water table. At wave rundown water moves in a predominant horizontal direction and exits the beach. The second factor that drives flow through sandy beaches is the flow of fresh groundwater from coastal aquifers. Under steady-state hydraulic boundary conditions (i.e., no waves or tide), incoming freshwater floats above a saltwater wedge (due to density

differences) and exits the beach (Glover, 1959; Henry, 1964; Frind, 1982; Galeati et al., 1994; Xue et al., 1996). The saltwater wedge acts as an impermeable boundary for the freshwater, forcing it to upcone towards the beach surface. The funneling effect due to the saltwater wedge causes the freshwater seaward velocity to increase when approaching the beach surface. The third factor that influences groundwater flow in beaches is the tide that results in a net seaward hydraulic gradient within the beach matrix (averaged over one tidal period) (Philip, 1973; Nielsen, 1990; Wrenn et al., 1997; Boufadel et al., 1998a). The seaward hydraulic gradient is due to the fact that the beach fills much faster than it drains resulting in an average beach water table that is above mean sea water level.

In this paper, we investigate the effects of buoyancy and tide on beach hydraulics and hydrodynamics (i.e., solute transport) using a laboratory beach setup and the numerical model MAR--for MARine-- (Boufadel et al., 1998b). The MAR model can simulate water flows in the saturated and the unsaturated zones of two-dimensional porous media taking into account the effect of salt concentration on water density and water viscosity (because saltwater is more viscous than freshwater). Such flows are designated here as density-and-viscosity dependent flows in two-dimensional variably-saturated media. For a detailed formulation and solutions of density-dependent flows in one-dimensional variably-saturated media, the reader is referred to the work by Boufadel *et al.* (1997).

The layout of the paper is as follows. First we present (briefly) the MAR model, its numerical implementation, and the laboratory setup. Next, an experiment simulating the effects of buoyancy and tide on the hydraulics and hydrodynamics of the laboratory beach is reported. The MAR model is used in conjunction with the data to provide water pressure and salinity information where no measurements are available. Our results highlight the shortcomings of approaches used in previous studies and provide guidelines for nutrient application on beaches.

The MAR model

The MAR model (Boufadel *et al.*, 1998b) solves simultaneously for the temporal (or steady-state) distribution

Table 1: Hydraulic and Hydrodynamic Parameters of the Laboratory Setup (Boufadel, 1998)

Parameter	Designation	Value/Units
K_{x0}	Saturated horizontal hydraulic conductivity	0.7 cm s ⁻¹
K_{z0}	Saturate vertical hydraulic conductivity	0.7 cm s ⁻¹
α^*	van Genuchten's (1980) sorptive parameter	0.185 cm ⁻¹
n	van Genuchten's (1980) uniformity coefficient	4.1[*]
S_r	van Genuchten residual saturation ratio	0.01[*]
S_0	Specific storage per unit fluid weight	0.0 cm ⁻¹
a_L	Longitudinal dispersivity	0.75 cm
a_T	Transverse dispersivity	0.75 cm

The experiments required the measurements of the positive pressures at the bottom and the salt concentration. The positive water pressure at the bottom was measured using pressure transducers (PT) (Model No. 1151AP, Fisher) that have a reading accuracy of about 2.0 mm. The PT's were placed 3.0 cm above the bottom of the tank and were logged by Strawberry Tree data software. The software

of water pressure and salinity, taking into account the effect of salt on water density and viscosity. The water flow equation is nonlinear in the unsaturated zone and is thus solved iteratively. The inter-dependence of the hydraulic conductivity, soil moisture, and pressure heads in the unsaturated zone is represented by the van Genuchten (1980) model although other models could be used in the MAR model (Boufadel et al., 1998a). The spatial discretization is done using the Galerkin finite element method with triangular elements, and time integration implemented using the modified Picard method with mass lumping (Celia et al., 1990). At each Picard iteration, the resulting system of linear equations is solved using a standard band LU decomposition method (Najem, 1982; Istok, 1989). Details of the modeling approach, model verification, and model validation are given by Boufadel et al. (1998a,b,c).

Laboratory beach

The facility used in the experiment consisted of an 8 m x 2 m x 0.6 m carbon steel tank, as diagrammed in Figure 1. One of the long vertical sides was made transparent by replacing the steel sheets with Plexiglas. The sand was positioned at a slope of 10% from a height of 115 cm to 65 cm and at 40 % slope from 65 cm to zero, which results in a total horizontal sand coverage of about 630 cm. A screen made of expanded steel and fine mesh was installed 30 cm from the left wall to hold the sand and to allow water passage. The open water behind the sand allows for a better capability of mixing, which provides a uniform freshwater distribution for [aquifer] simulations. Two "sacrificial" zinc plates were placed in the tank on both ends to reduce steel corrosion from the tank. Zinc was selected because it has a higher oxidation potential than steel.

The sand used in the tank was coarse with a median size of 1.0 mm and a very narrow particle size distribution, varying between 0.8 and 1.2 mm. These sand properties resulted in a very little sand transport by suspension. The sand hydraulic and hydrodynamic parameters are reported in Table 1.

was used also to control the water level in the tank by sending the appropriate electronic signal to the inflow and the outflow pumps.

The concentration of the salt was measured by conductivity meters (CM) (CDCN 108, Omega Engineering) that measure the electrical conductivity of the water solution, which varies with the salt concentration. The

CM's were logged to a CR10 data logging software (Rocktest, Inc., Plattsburg, NY). The accuracy of the CM's was about 5% of the measured salt concentration. The locations of the CMs along the length of the tank are given in Figure 1. The horizontal distances of the CM's from the Plexiglas wall were different to ensure that a sensor does not

alter greatly the flow lines to another one along the general flow direction. The distances from the Plexiglas wall can be found in the work by Boufadel (1998). The data from all sensors were logged at an interval of 30 s.

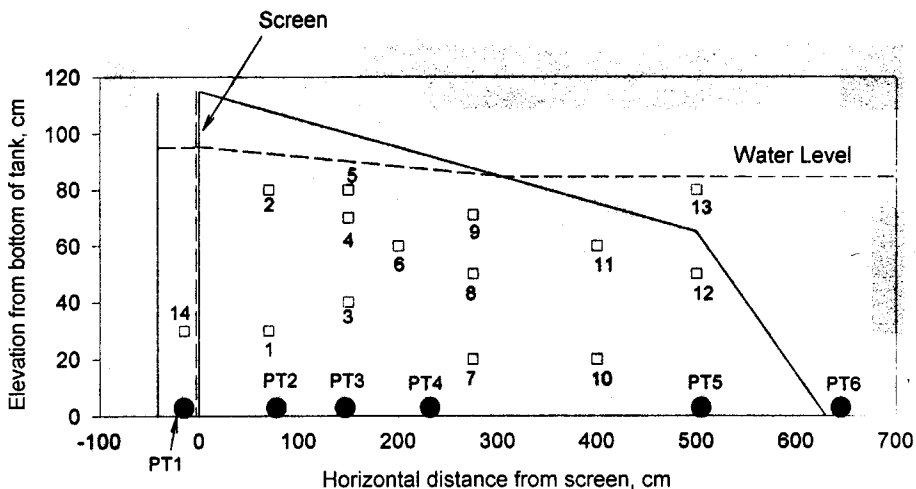


Figure 1. Laboratory tank and location of sensors. The solid squares represent the Conductivity Meters, CM.

Experimental and numerical investigation

The objective was to determine the effects of buoyancy and tide on nutrient transport within a coarse sandy beach. An experiment was conducted to simulate the combined effects of tide and buoyancy on beach hydraulics and hydrodynamics. The maximum salt concentration was 32.0 g/L (salinity at the coasts of the continental U.S.).

Experiment. The experiment was started by inducing a steady state water pressure and concentration distribution in the tank. The water pressures at PT1 and PT6 were set at 85 cm and 70 cm, respectively. The saltwater was circulated through the tank until a uniform salt concentration of 32 g/L was obtained. Then freshwater (tap water) was introduced behind (to the left of) the screen under the same steady state hydraulic regime. Because of the difference in water head between PT1 and PT6, the freshwater was propagated in the beach towards the sea causing a reduction of the salinity in the beach. The tidal cycle was started when the concentration at CM9 dropped to 1/3 of its initial value. The tidal level was controlled by the reading at PT6, which was set to vary between 70 cm and 95 cm. Based upon the grain size of the sand in the mesocosm and the wave height and tidal amplitude able to be generated in the tank, dimensionless analysis was used to determine a tidal period that would simulate the conditions observed in a previous field study at Slaughter Beach, Delaware (Wrenn *et al.*, 1997). This tidal period was about 20 minutes (see

computation method given under the Section entitled Scaling).

The minimum reading at PT1 was set at 85 cm (i.e., freshwater is introduced whenever the reading at PT1 dropped below 85 cm). A mixer was running continuously in the open water at the sea side to simulate the high mixing in the sea.

The freshwater, whose salinity varied between 0.15 g/L and 0.2 g/L during the course of the experiments, was applied uniformly across the width of the tank from a perforated tube in the low end behind the screen. The injected freshwater contained air bubbles, which increased the mixing in the open water behind the screen. To investigate the extent of the mixing, salinity measurements were taken along the depth behind the screen using a multiport sampling well (Wrenn *et al.* 1997; Boufadel, 1998). The salt concentration was found to be the same throughout the water column. Thus, the open water area behind the screen was considered completely mixed when water was introduced this way.

Prior to the tidal action, a seepage face of length about 15 cm was observed at the beach surface. The length of the seepage face varied during the tidal cycle. It disappeared for $PT6 \geq 85$ cm and reached about 30 cm at low tide.

The observed pressure heads and concentrations are shown in Fig. 2. Buoyancy effects were evident prior to tidal action when comparing the salinity at the sensors CM7, CM8, and CM9, which are on the same vertical. The delay in the arrival of the freshwater plume at CM7 with respect to CM9 was about 0.3 hr.

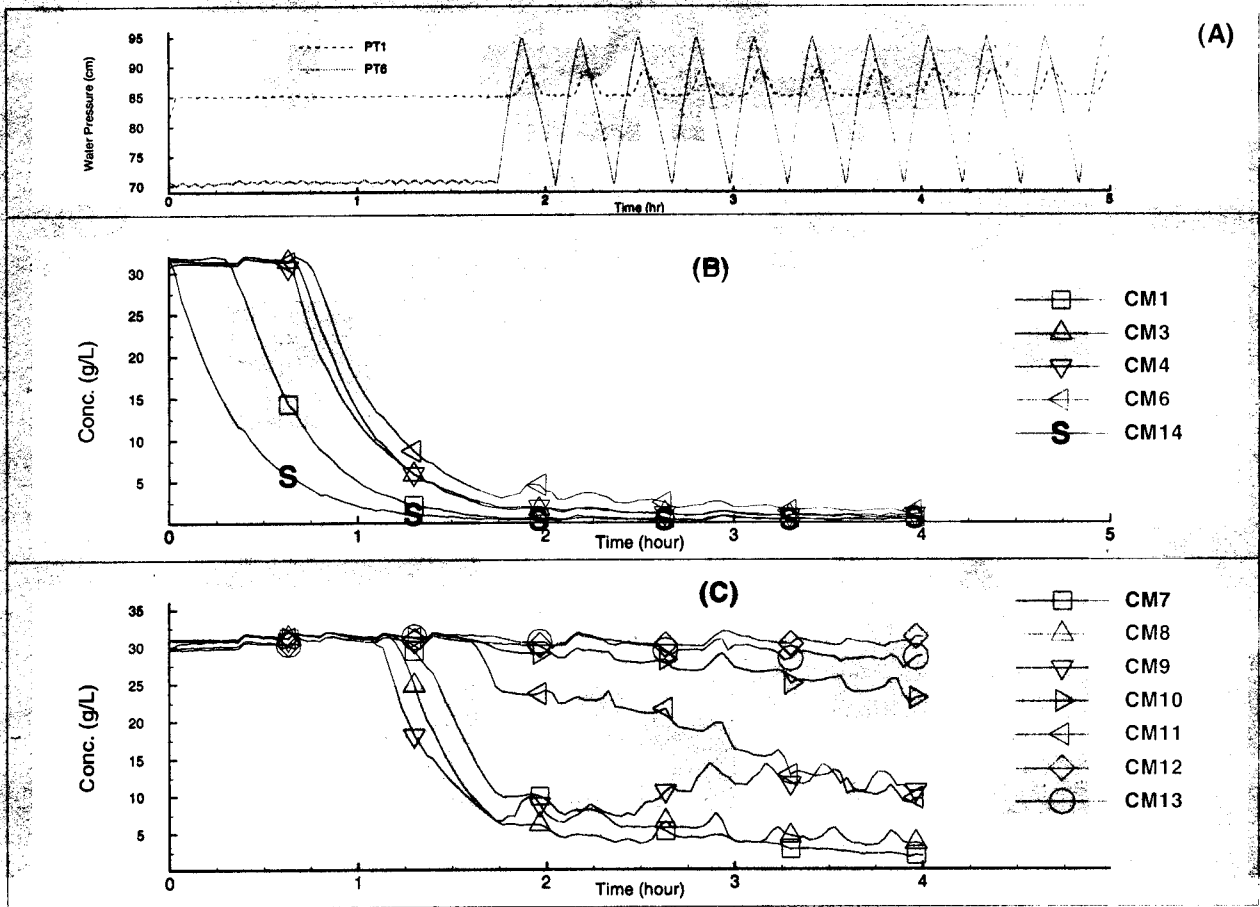


Figure 2. Observed water pressures and concentrations in the presence of density-dependence. All results are obtained at a 30 s interval.

Under tidal action (Figure 2c), a rise in the salinity at CM9 is clearly observed. A discussion on this observation is provided later in the manuscript.

Modeling. Due to the dependence of water flow on the salt concentration, a steady-state hydraulic regime does not exist even if the hydraulic boundary conditions are at steady state. The flow and transport equations are coupled.

The MAR model was run with the parameters listed in Table 1 to simulate this experiment. Modeling results were essentially unchanged when concentration-engendered viscosity effects were neglected. A similar finding was reported by Galeati et al. (1992) in application to saltwater

intrusions in natural systems. Schincariol et al. (1997) argued that at typical groundwater velocities, concentration-engendered viscosity effects are negligible in comparison to concentration-engendered density effects. A good agreement was obtained between the simulated and observed results, as reported by Boufadel et al. (1998c).

Simulation results of the model are plotted in Fig. 3 for two simulation times. The times were selected to show the dependent variables (pressure, concentration, Darcy flux) just before the tidal cycle and close to a high tide, a few cycles later.

